AIMS Mathematics, 10(8): 18838–18860.
DOI:10.3934/math.2025842
Received: 27 March 2025
Revised: 17 June 2025
Accepted: 12 August 2025
Published: 20 August 2025

http://www.aimspress.com/journal/Math

Research article

The Markov-switching threshold BLGARCH model

R. Alraddadi*

Department of Mathematics and Statistics, College of Science in Yanbu, Taibah University, Madinah 46423, Saudi Arabia

* **Correspondence:** Email: rmraddadi@taibahu.edu.sa.

Abstract: This paper introduces a novel and enhanced class of Markov-switching threshold BLGARCH (MS-TBLG) models designed to better capture the intricate behavior of financial time series. By incorporating both a threshold mechanism and interaction effects between returns and their conditional volatility, the proposed framework significantly improves upon traditional Markov-switching BLGARCH (MS-BLG) models. This structure allows for a more flexible representation of regime-dependent volatility, particularly in modeling asymmetric effects such as the leverage effect—where negative and positive shocks have differing impacts across regimes. We established key conditions that guarantee the stationarity, causality, and ergodicity of the MS-TBLG process, and derived analytical expressions for its power covariance functions, taking the threshold effect into account. To estimate the model parameters efficiently, we developed a generalized method of moments (GMM) procedure specifically adapted to the complexity of Markov-switching dynamics. This approach utilizes moment conditions derived from the power-transformed squared process, ensuring consistent estimation despite the presence of unobserved regime shifts. The effectiveness and robustness of the estimation strategy were validated through extensive Monte Carlo simulations. Finally, the model's practical relevance was illustrated through an empirical application to oil price data, showcasing its effectiveness in capturing regime-switching behavior and complex volatility dynamics.

Keywords: GARCH model; bilinear model; Markov-switching model; GMM; stationarity; threshold effect
Mathematics Subject Classification: Primary 62M10; Secondary 62M05

1. Introduction and motivation

The pioneering works by Engle [1] and Bollerslev [2] introduced the generalized autoregressive conditional heteroskedasticity (GARCH) models, drawing significant attention from researchers and

analysts. GARCH models are essentially discrete-time stochastic processes that address volatility clustering in time series data, such as stock returns and exchange rates. Formally, a GARCH process $(T_\tau)_{\tau\in\mathbb{Z}}$ is defined as:

$$T_\tau = \sigma_\tau \rho_\tau, \tag{1.a}$$

where $(\rho_\tau)_{\tau\in\mathbb{Z}}$ is an independent and identically distributed (i.i.d.$(0,1)$) innovation process, and σ_τ is a volatility function dependent on past observations and volatilities, given by: $\sigma_\tau = \varphi(\sigma_{\tau-u}, T_{\tau-v}, u = 1, ..., r_1, v = 1, ..., r_2)$, for a specific measurable function defined on the real line. The GARCH model's effectiveness in modeling stylized facts, such as the persistence of volatility, leptokurtosis, and heavy tails has made it a powerful tool for modeling financial time series. However, traditional GARCH models fall short when dealing with asymmetric data exhibiting leverage effects, where negative shocks have a larger impact on volatility than positive ones. This limitation has driven researchers to explore advanced specifications like generalized quadratic, threshold, Glosten–Jagannathan–Runkle (GJR), logarithmic, exponential, and asymmetric power (G)ARCH models. Among these advancements, the bilinear-GARCH (BLG) model proposed by Storti and Vitale [3] represents a significant extension. The BLG model incorporates bilinearity into the volatility structure, formulated as:

$$\sigma_\tau^2 = p_0 + \sum_{u=1}^{r_2} p_u T_{\tau-u}^2 + \sum_{v=1}^{r_1} q_v \sigma_{\tau-v}^2 + \sum_{w=1}^{r_1\wedge r_2} s_w T_{\tau-w}\sigma_{\tau-w}. \tag{1.b}$$

The motivation behind the BLG model is to address the inadequacies of traditional GARCH models in reflecting the intricacies of real-world financial data. BLG models excel in capturing asymmetries in the conditional variance of financial and economic time series through interactions between past shocks and volatilities. Empirical finance has established that the volatility of many financial assets exhibits asymmetry. Specifically, stock price fluctuations are often inversely correlated with changes in volatility, indicating that volatility typically increases more following negative shocks compared to equivalent positive shocks (see [4]). Moreover, the BLG model uniquely addresses two critical properties of non-linear time series: volatility clustering and leverage effects. Previous studies on GARCH models have primarily focused on capturing empirical characteristics such as volatility clustering between returns and conditional variance. While some models address leverage effects, they often fail to simultaneously capture both volatility clustering and leverage effects within a non-Gaussian framework. The BLG model, therefore, provides a valuable tool for capturing these essential properties in high-frequency financial data, such as daily stock returns.

Building upon the foundational insights provided by the BLG model, the threshold BLG (TBLG) model introduces significant enhancements to volatility modeling by integrating both threshold and bilinear effects. The BLG model effectively captures asymmetries and leverage effects in volatility, addressing many shortcomings of traditional GARCH models. However, financial time series often exhibit more complex asymmetric patterns, where volatility σ_τ depends on the signs of past values (see [5]). To address these patterns, Choi et al. [6] proposed the TBLG model, which builds upon the BLG framework by incorporating the "threshold effect" alongside the bilinear structure of (1.a)–(1.b). The TBLG (1,1) model enhances the BLG (1,1) approach by introducing two sources of asymmetry: threshold asymmetry and shift asymmetry. The model is defined as:

$$\sigma_\tau^2 = p_0 + \left(p_1^{(1)}(T_{\tau-1}^+)^2 + p_1^{(2)}(T_{\tau-1}^-)^2\right) + q_1\sigma_{\tau-1}^2 + \left(s_1^{(1)}T_{\tau-1}^+ + s_1^{(2)}T_{\tau-1}^-\right)\sigma_{\tau-1}, \tag{1.c}$$

where $T^{\pm} = (\pm T) \vee 0$. Observe that $T = T^{+} - T^{-}$ and $|T| = T^{+} + T^{-}$. In this model, $s_1^{(i)}$, $i = 1, 2$, can take any values within $\mathbb{R}$ while $p_0 \in \mathbb{R}_{*}^{+}$ and the parameters $p_1^{(1)}$, $p_1^{(2)}$, and q_1 are constrained to be positive. To prevent trivial cases, we exclude scenarios where both $p_1^{(i)}$, $i = 1, 2$, are zero. Specifically, when $p_1^{(1)} = p_1^{(2)}$ and $s_1^{(1)} + s_1^{(2)} = 0$, the TBLG model simplifies to the BLG model, which lacks threshold effects. Additionally, if $s_1^{(1)} = s_1^{(2)} = 0$, the TBLG model reduces to the threshold model (TGARCH).

While these advanced models significantly improve over standard BLG models, they remain single-regime systems, lacking the flexibility to accommodate regime shifts in volatility dynamics. This limitation has been addressed in the literature through Markov-switching GARCH (MS-GARCH) models, which allow parameters to vary across latent regimes. In this context, several seminal contributions stand out: [7] introduced a regime-switching model for interest rates that incorporates mean reversion and conditional heteroskedasticity. [8] improved volatility forecasting in GARCH models by introducing regime-dependent persistence, demonstrating superior out-of-sample performance in exchange rate forecasting. [9] proposed a more tractable MS-GARCH framework that facilitates estimation while effectively capturing volatility dynamics across different regimes. These works laid the theoretical foundation for regime-switching extensions of asymmetric volatility models. Markov-switching models address this limitation by changing model parameters using a hidden Markov process. This approach captures structural breaks and regime changes in financial data more effectively. These works laid the theoretical foundation for regime-switching extensions of asymmetric volatility models. Abramson and Cohen [10] established the stationarity properties of Markov-switching GARCH processes, providing a fundamental framework for studying regime-dependent dynamics, while Cavicchioli [11, 12] further examined higher-order moments and volatility behavior, demonstrating their effectiveness in capturing the effects of economic recessions and extreme events such as pandemics. Building on this line of research, Ghezal and Alzeley [13] investigated periodic threshold autoregressive stochastic volatility models, and Ghezal et al. [14] introduced Markov-switching threshold stochastic volatility models that explicitly account for regime changes. Complementary to these studies, Ghezal [15] proposed a spectral representation of Markov-switching bilinear processes, thereby extending the analytical toolkit for analyzing such models. More recent contributions by Ghezal and Zemmouri [16] explored Markov-switching autoregressive stochastic volatility processes, while in another study [17], they analyzed asymmetric log-GARCH models with regime-switching features, establishing important results on stationarity and estimation. Their most recent work [18] developed M-estimation methods for periodic threshold GARCH models, proving both consistency and asymptotic normality, which reinforces the robustness of inference in these contexts. To achieve greater flexibility in modeling volatility persistence, Ghezal et al. [19] integrated volatility with time-homogeneous Markov chain states, which are unobservable and control the dynamics of volatility with a finite state space $\mathbb{E} = \{1, \ldots, e\}$ for potential regimes. This approach has led to the development of a broader class of non-homogeneous conditionally asymmetric models. The resulting model is referred to as the Markov-switching BLG (MS-BLG$(r_1, r_2, r_1 \wedge r_2)$) model, defined as:

$$\sigma_\tau^2 = p_0(\delta_\tau) + \sum_{u=1}^{r_2} p_u(\delta_\tau) T_{\tau-u}^2 + \sum_{v=1}^{r_1} q_v(\delta_\tau) \sigma_{\tau-v}^2 + \sum_{w=1}^{r_1 \wedge r_2} s_w(\delta_\tau) T_{\tau-w} \sigma_{\tau-w}, \tag{1.d}$$

where $(\delta_\tau)_{\tau \in \mathbb{Z}}$ is a stationary, irreducible, and aperiodic Markov chain. This chain is defined by its $m-$step transition probabilities matrix $\mathbb{M}^{(m)} = \left(M_{lk}^{(m)}\right)_{(l,k) \in \mathbb{E} \times \mathbb{E}}$ where $M_{lk}^{(m)} = P(\delta_\tau = k | \delta_{\tau-m} = l)$. The

chain's unconditional distribution is denoted by $\underline{\Lambda}' = (\lambda(1), ..., \lambda(e))$, where $\lambda(l) = P(\delta_0 = l) > 0$, $l \in \mathbb{E}$, and it satisfies $\underline{\Lambda}' = \underline{\Lambda}'\mathbb{M}$. Furthermore, we assume that ρ_τ in (1.a) is independent of the sequence $\left\{\left(T_{j-1}, \delta_\tau\right), j \leq \tau\right\}$. This model introduced by Ghezal et al. [19] enhanced the traditional BLG models by allowing the model's parameters to switch according to the hidden Markov states. This switching mechanism captures the regime-dependent dynamics of volatility, making the model more adaptable to different market conditions and volatility regimes. By incorporating Markov chain states, the MS-BLG model provides a richer and more flexible framework for modeling financial time series data, which often exhibit complex and evolving volatility structures. This advanced specification not only addresses the limitations of standard BLG models in capturing sudden shifts in volatility but also improves the accuracy of volatility forecasts by considering the potential regime changes.

By combining the bilinear and threshold structures of Eqs (1.a) and (1.c) with the Markov-switching mechanism of Eq (1.d), the proposed model provides a comprehensive and flexible framework for modeling complex financial time series. This unified specification captures not only short-term asymmetries and nonlinear effects but also structural shifts and persistent changes in volatility regimes, thereby enhancing the accuracy of volatility forecasting and risk management. In particular, the Markov-switching threshold bilinear GARCH (MS-TBLG) model integrates two complementary sources of regime dependence: threshold effects, governed by observable return components such as $T^{\pm}_{\tau-1}$, which capture sign-based asymmetries including leverage effects; and Markov-switching dynamics, driven by the latent state variable δ_τ, which models persistent, unobservable shifts in the market environment (e.g., transitions between high- and low-volatility regimes). These two components are conceptually and statistically distinct: threshold effects reflect immediate market responses to positive or negative shocks, while Markov-switching captures underlying state-dependent structural evolution. The combination allows for a richer representation of real-world financial processes, where short-term asymmetries and long-term regime transitions often coexist. We now introduce the MS-TBLG model:

$$\sigma^2_\tau = p_0(\delta_\tau) + \sum_{u=1}^{r_2}\left(p^{(1)}_u(\delta_\tau)(T^+_{\tau-u})^2 + p^{(2)}_u(\delta_\tau)(T^-_{\tau-u})^2\right) + \sum_{v=1}^{r_1} q_v(\delta_\tau)\sigma^2_{\tau-v} + \sum_{w=1}^{r_1\wedge r_2}\left(s^{(1)}_w(\delta_\tau)T^+_{\tau-w} + s^{(2)}_w(\delta_\tau)T^-_{\tau-w}\right)\sigma_{\tau-w}. \tag{1.e}$$

In this model, the coefficients vary with the regime, allowing the model to adapt to different volatility regimes. For $l \in \mathbb{E}$, the coefficients $\left(p_0(l), p^{(i)}_u(l), i = 1, 2, u = 1, ..., r_2\right)$, $(q_v(l), v = 1, ..., r_1)$ are positive with $p_0(l) \in \mathbb{R}^+_*$. Additionally, $\left(s^{(i)}_w(l), i = 1, 2, w = 1, ..., r_1 \wedge r_2\right)$ represent the asymmetry coefficients that control the leverage effect. Given that σ_τ denotes a conditional variance, it is required to be strictly positive. Thus, we will adopt the following positivity condition for the entirety of this paper: For any given time τ, $P(\sigma_\tau \in \mathbb{R}^+_*) = 1$. In a manner similar to the approach used by Storti and Vitale [3] and Choi et al. [6], a sufficient condition for ensuring the positivity of σ^2_τ is given by the inequalities: $\sum_{i=1}^{2}\left(s^{(i)}_w(l)\right)^2 < 4\left(\prod_{i=1}^{2} p^{(i)}_w(l) + q_w(l)\sum_{i=1}^{2} p^{(i)}_w(l)\right)$ and $\sum_{i=1}^{2}\sum_{\substack{j=1\\ i\neq j}}^{2} p^{(i)}_w(l)\left(s^{(j)}_w(l)\right)^2 < 4q_w(l)\prod_{i=1}^{2} p^{(i)}_w(l)$ for all $l \in \mathbb{E}$ and $w = 1, ..., r_1 \vee r_2$.

The MS-TBLG model encompasses several models previously studied as particular instances. Specifically, the standard TBLG model is derived by considering the Markov chain operates under a

single regime (see [6]). Additionally, the MS-TGARCH model is achieved by imposing the constraint $p_u^{(1)}(.) \pm p_u^{(2)}(.) = 0$ and $s_w^{(1)}(.) = s_w^{(2)}(.) = 0$ for all u, w in (1.e) (see [11]). The MS-BLG model results from applying the constraint $p_u^{(1)}(.) \pm p_u^{(2)}(.) = 0$ and $s_w^{(1)}(.) + s_w^{(2)}(.) = 0$ for all u, w in (1.e) (see [19]). Furthermore, the independent-switching MS-TBLG model is obtained when the chain (δ_τ) is an independent Markov chain (see [20]).

The structure of this paper is as follows. Section 2 presents the theoretical properties of the MS-TBLG model, including conditions for stationarity, causality, and ergodicity. Section 3 derives the moment and covariance for the power MS-TBLG model. Section 4 outlines the GMM estimation procedure tailored for the MS-TBLG model. Section 5 validates the estimation method through Monte Carlo simulations. Section 6 applies the MS-TBLG model to real-world data, specifically the exchange rate between the Algerian Dinar and the Euro, demonstrating the model's practical applicability. Finally, Section 7 concludes with a summary of the findings and potential directions for future research.

2. Stationarity

In this section, we outline certain conditions that guarantee the existence of strict, second-order stationary, causal, and ergodic solutions for the MS-TBLG model. Consequently, as with many time series models, it is advantageous to express the MS-TBLG model in an equivalent Markovian representation to facilitate easier analysis. To accomplish this, we employ vector notations $\underline{T}_\tau^{\pm(2)} := ((T_\tau^{\pm})^2, ..., (T_{\tau-r_2+1}^{\pm})^2)'$, $\underline{\sigma}_\tau^{(2)} := (\sigma_\tau^2, ..., \sigma_{\tau-r_1+1}^2)'$, $\underline{Y}_\tau^{\pm(2)} := (T_\tau^{\pm}\sigma_\tau, ..., T_{\tau-r_1\wedge r_2+1}^{\pm}\sigma_{\tau-r_1\wedge r_2+1})'$, $\underline{\Upsilon}_\tau := \left(\left(\underline{T}_\tau^{+(2)}\right)', \left(\underline{T}_\tau^{-(2)}\right)', \left(\underline{\sigma}_\tau^{(2)}\right)', \left(\underline{Y}_\tau^{+(2)}\right)', \left(\underline{Y}_\tau^{-(2)}\right)'\right)'$, and $\underline{\Pi}(\delta_\tau, \rho_\tau) := \underline{p}_{0,1}(\delta_\tau)(\rho_\tau^+)^2 + \underline{p}_{0,r_2+1}(\delta_\tau)(\rho_\tau^-)^2 + \underline{p}_{0,2r_2+r_1+1}(\delta_\tau)\rho_\tau^+ + \underline{p}_{0,2r_2+r_1+r_1\wedge r_2+1}(\delta_\tau)\rho_\tau^- + \underline{p}_{0,2r_2+1}(\delta_\tau)$, where, $\underline{p}_{0,k}(\delta_\tau)$ has its kth entry as $p_0(\delta_\tau)$, with all other elements being 0. The aforementioned steps allow us to transition from the scalar representation of Eqs (1.a) and (1.e) to the following vectorial representation: $T_\tau^2 = \underline{L}\underline{\Upsilon}_\tau$ or $\sigma_\tau^2 = \underline{K}\underline{\Upsilon}_\tau$ and

$$\underline{\Upsilon}_\tau = \Psi(\delta_\tau, \rho_\tau)\,\underline{\Upsilon}_{\tau-1} + \underline{\Pi}(\delta_\tau, \rho_\tau), \tag{2.a}$$

where $\underline{L} := \left(\underbrace{1,0,...,0}_{r_2-times}, \underbrace{1,0,...,0}_{(r_2+r_1+2r_1\wedge r_2)-times}\right)$, $\underline{K} := \left(\underbrace{0,...,0}_{2r_2-times}, \underbrace{1,0,...,0}_{(r_1+2r_1\wedge r_2)-times}\right)$, $\Psi(\delta_\tau, \rho_\tau) = \sum_{k=1}^{5} \Psi^{(k)}(\delta_\tau)\,\rho_\tau^{(-1)^{k+1}[k/2]}$, and the matrices $\left(\Psi^{(k)}(\delta_\tau), k = 1, ..., 5\right)$ are square matrices explicitly and straightforwardly derived from the parameters of Eq (1.e).

Remark 2.1. *The process $\left(\underline{\Upsilon}_\tau\right)_{\tau\in\mathbb{Z}}$ is not a Markov chain; however, the combined process $\left(\left(\underline{\Upsilon}_\tau', \delta_\tau\right)'\right)_{\tau\in\mathbb{Z}}$ forms a Markov chain on $\mathbb{R}^h \times \mathbb{E}$. This distinction is crucial because while $\underline{\Upsilon}_\tau$ alone lacks the Markov property, the augmentation with the state variable δ_τ ensures that the combined process satisfies the Markov condition. This means that the future behavior of the process $\left(\left(\underline{\Upsilon}_\tau', \delta_\tau\right)'\right)_{\tau\in\mathbb{Z}}$ depends only on its current state, not on the sequence of events that preceded it. This property facilitates the analysis and modeling of the system, allowing for more accurate predictions and understanding of its dynamics.*

Remark 2.2. *Through the scalar representation (1.a) and (1.e) and the vectorial representation (2.a), it becomes evident that there is an equivalence in the existence of causal, stationary, and ergodic solutions for both representations. Additionally, the vectorial representation captures an autoregressive vector with coefficients that vary according to a Markov chain. This equivalence is*

crucial as it ensures that the solutions derived from either representation maintain the same properties, allowing a consistent analysis of the system's behavior. The vectorial form, in particular, facilitates the interpretation and manipulation of the model, providing a more robust framework for understanding the dynamics influenced by the Markov process.

The top-Lyapunov exponent is crucial for analyzing strict stationarity, and the subsequent theorem guarantees the existence of a unique solution that is causal, strictly stationary, ergodic, and bounded in probability. This ensures that the solution is well-behaved and adheres to essential statistical properties, making it suitable for both theoretical analysis and practical applications.

Theorem 2.1. *Consider the Eq (2.a). A unique solution that is causal, strictly stationary, ergodic, and bounded in probability is provided as:*

$$\underline{\Upsilon}_{\tau} = \sum_{j\geq 0}^{\infty} \left(\prod_{i=0}^{j-1} \Psi\left(\delta_{\tau-i}, \rho_{\tau-i}\right) \right) \underline{\Pi}\left(\delta_{\tau-j}, \rho_{\tau-j}\right), \tag{2.b}$$

where $\Psi(\delta_{\tau}, \rho_{\tau})$ is a real-valued square matrix encoding the autoregressive dynamics under each threshold–regime pair $(\delta_{\tau}, \rho_{\tau})$, and $\underline{\Pi}(\delta_{\tau}, \rho_{\tau})$ is an innovation vector representing random shocks specific to each pair $(\delta_{\tau}, \rho_{\tau})$. This solution exists if and only if the Lyapunov exponent $\mathcal{L}_{\Psi}$, related to the sequence of random matrices $\Psi := (\Psi(\delta_{\tau}, \rho_{\tau}))_{\tau\in\mathbb{Z}}$, satisfies:

$$\mathcal{L}_{\Psi} := \lim_{j\to\infty} E\left\{ \log \left\| \prod_{i=0}^{j-1} \Psi\left(\delta_{\tau-i}, \rho_{\tau-i}\right) \right\|^{1/j} \right\} < 0. \tag{2.c}$$

Furthermore, if $\underline{K}$ is a constant, invertible transformation matrix, then the process $\left(\underline{K\Upsilon}_{\tau}\right)_{\tau\in\mathbb{Z}}$ represents the unique solution to Eq (1.e) that shares the same probabilistic characteristics as $\left(\underline{\Upsilon}_{\tau}\right)_{\tau\in\mathbb{Z}}$.

Proof. By leveraging the fundamental properties of the original process $((\delta_{\tau}, \rho_{\tau}))_{\tau\in\mathbb{Z}}$, given that this process is strictly stationary and ergodic, it ensures that any functionally dependent process, such as $\left(\left(\Psi(\delta_{\tau}, \rho_{\tau}), \underline{\Pi}(\delta_{\tau}, \rho_{\tau})\right)\right)_{\tau\in\mathbb{Z}}$, will also retain these properties. The structure of Eq (2.a) is similar to those analyzed by Bougerol and Picard [21]. Their work, through the finiteness of $E\left\{\max\left(\log\|\Psi(\delta_{\tau}, \rho_{\tau})\|, 0\right)\right\}$ and $E\left\{\max\left(\log\left\|\underline{\Pi}(\delta_{\tau}, \rho_{\tau})\right\|, 0\right)\right\}$, demonstrated that such conditions lead to strict stationarity and ergodicity in the transformed process. Consequently, by aligning with their framework and utilizing the provided moment conditions, we confirm that Eq (2.a) indeed possesses the same strict stationarity and ergodicity, thereby completing the proof. □

Remark 2.3. *The Lyapunov exponent $\mathcal{L}_{\Psi}$ stated in the preceding theorem is well-defined and does not depend on the particular choice of matrix norm, since all norms are equivalent in finite-dimensional spaces. For clarity, we adopt the $\mathbb{L}_1$-norm, defined as: $\|B\| = \sum_{i,j}|B(i,j)|$. This norm satisfies the essential submultiplicative property.*

Remark 2.4. *To establish a sufficient condition for $\mathcal{L}_{\Psi} < 0$, one can benefit from either condition $E\left\{\log\left\|\prod_{i=0}^{j-1}\Psi(\delta_{\tau-i}, \rho_{\tau-i})\right\|\right\} < 0$ or $E\left\{\left\|\prod_{i=0}^{j-1}\Psi(\delta_{\tau-i}, \rho_{\tau-i})\right\|\right\} < 1$. Specifically, Jensen's inequality provides a framework for proving that if the expectation of the norm of the matrix product, $\Psi(\delta_{\tau}, \rho_{\tau})$, is strictly*

less than 1*, then* $\mathcal{L}_\Psi$ *must indeed be negative. This approach effectively shows that under these conditions, a negative Lyapunov exponent is guaranteed and thus verifies the strict stationarity and efficiency of the process.*

Remark 2.5. *In the analysis of MS-TBLG processes, it is crucial to understand the relationship between local and global stationarity. Unlike the case with Markov-switching models, where local stationarity within each regime is a sufficient condition for achieving global stationarity, but is not a necessity, the MS-TBLG process presents a distinct scenario. For MS-TBLG models, global stationarity can be achieved if local stability persists within each system, although global stability does not automatically imply local stability. This distinction highlights the complexity of stationarity conditions in MS-TBLG models. For a comprehensive exploration of these concepts, see the work of Ghezal [22], which provides detailed discussions on how these stationarity conditions interact and impact the modeling of time series.*

Remark 2.6. *Our decision to adopt a two-state (positive/negative shock) threshold structure within the MS-TBLG framework is grounded in both theoretical and empirical considerations. Empirically, the literature suggests that sign-based asymmetry—commonly referred to as the leverage effect—is the predominant form of asymmetry observed in financial markets. Structurally, the Markovian component of the model, consisting of* $e \geq 2$ *hidden states, enables the capture of complex structural shifts and unobserved market regimes. As demonstrated in Eq* (*1.e*)*, the threshold parameters* $p_u^{(i)}(\delta_\tau)$ *and* $s_w^{(i)}(\delta_\tau)$ *vary across the Markovian states, thereby adding flexibility without increasing the number of threshold partitions. Moreover, although multi-threshold models (e.g., [23]) are theoretically appealing, they introduce substantial computational complexity during estimation and, according to our preliminary findings, do not yield significant improvements in predictive accuracy. Thus, the choice of a simplified two-state threshold design contributes to interpretability and computational tractability, while retaining strong predictive performance. Nevertheless, we acknowledge that extending the model to allow for multiple thresholds or soft regime transitions remains a promising avenue for future research. Achieving this would require revising the theoretical conditions for stationarity. Overall, the current model reflects a deliberate balance between generality and computational efficiency, and serves as a flexible foundation for potential future extensions informed by recent developments in generalized threshold modeling.*

Example 2.1. *For the MS-TBLG model when* $r_1 = r_2 = 1$*, a critical aspect in ensuring the existence of a unique, causal, strictly stationary, and ergodic solution is the evaluation of specific conditions related to the model parameters. One such sufficient condition can be expressed as:*

$$E\left\{\log\prod_{k=1}^{e}\left|p_1^{(1)}(k)(\rho_1^+)^2+p_1^{(2)}(k)(\rho_1^-)^2+s_1^{(1)}(k)\rho_1^++s_1^{(2)}(k)\rho_1^-+q_1(k)\right|^{\lambda(k)}\right\}<0. \tag{2.d}$$

This implies that the model can remain strictly stationary even in the presence of potentially explosive regimes, where:

$$E\left\{\log\left|p_1^{(1)}(k_0)(\rho_1^+)^2+p_1^{(2)}(k_0)(\rho_1^-)^2+s_1^{(1)}(k_0)\rho_1^++s_1^{(2)}(k_0)\rho_1^-+q_1(k_0)\right|^{\lambda(k_0)}\right\}>0.$$

Table 1 outlines Condition (2.*d*) *for certain instances of the MS-TBLG model when* $r_1 = r_2 = 1$.

Table 1. Summary of Condition (2.d) for strict stationarity in MS-TBLG submodels when $r_1 = r_2 = 1$.

Models	Condition (2.d)
TBLG	$E\left\{\log\left\|p_1^{(1)}(1)(\rho_1^+)^2 + p_1^{(2)}(1)(\rho_1^-)^2 + s_1^{(1)}(1)\rho_1^+ + s_1^{(2)}(1)\rho_1^- + q_1(1)\right\|\right\} < 0$
MS-BLG	$E\left\{\log\prod_{k=1}^{e}\left\|p_1^{(1)}(k)\rho_1^2 + s_1^{(1)}(k)\rho_1 + q_1(k)\right\|^{\lambda(k)}\right\} < 0$
MS-GARCH	$E\left\{\log\prod_{k=1}^{e}\left\|p_1^{(1)}(k)\rho_1^2 + q_1(k)\right\|^{\lambda(k)}\right\} < 0$

Strict stationarity, which requires the entire distribution of a time series to remain unchanged under time shifts, is a rigorous and often challenging condition. In contrast, second-order stationarity, also known as weak stationarity, focuses on the constancy of the mean and variance over time, and the dependence of covariance solely on the time lag. This more relaxed condition simplifies the analysis and is widely applicable in practical modeling. The following result provides the condition for achieving second-order stationarity.

Theorem 2.2. *For Eq* (2.*a*)*, consider the non-random square matrix* Ψ *defined as* $\Psi := (\Psi(k) = E\{|\Psi(k,\rho_\tau)|\}, k \in \mathbb{E})$*. Suppose the spectral radius condition:*

$$\rho^*(\mathbb{M}(\Psi)) < 1, \tag{2.e}$$

is satisfied, where $\mathbb{M}(\Psi)$ *is defined as:* $\mathbb{M}(\Psi) = \begin{pmatrix} M_{11}\Psi(1) & \dots & M_{e1}\Psi(1) \\ \vdots & \dots & \vdots \\ M_{1e}\Psi(e) & \dots & M_{ee}\Psi(e) \end{pmatrix}$ *for any collection of non-random matrices* $\Psi := \{\Psi(k), k \in \mathbb{E}\}$*, which encodes both the dynamic effects and the switching structure of the system. Under this condition, Eqs* (*1.a*)*–*(*1.e*) *admit a unique second-order stationary solution, which is represented as* $\left(\underline{K\Upsilon}_\tau\right)^{1/2}\rho_\tau$*. Here, the series representation for* $\underline{\Upsilon}_\tau$ *as defined in* (2.*b*) *converges almost surely in an absolute sense, as well as in the* $\mathbb{L}_1$ *space. Additionally, this solution exhibits strict stationarity and ergodicity.*

Proof. To establish Theorem 2.2, we employ the methodology analogous to Francq et al. [24]. Initially, by iterating Eq (2.a) backwards, we derive for any $j - 1 \geq 0$, the following expression:

$$\underline{\Upsilon}_\tau = \Omega_\tau(j)\underline{\Upsilon}_{\tau-j-1} + \underline{\Phi}_j(\tau), \tag{2.f}$$

where $\Omega_\tau(j) = \prod_{i=0}^{j-1}\Psi(\delta_{\tau-i},\rho_{\tau-i})$ and $\underline{\Phi}_j(\tau) = \sum_{s=0}^{j-1}\left(\prod_{i=0}^{s-1}\Psi(\delta_{\tau-i},\rho_{\tau-i})\right)\underline{\Pi}(\delta_{\tau-s},\rho_{\tau-s})$. To confirm that the series (2.b) is properly defined in the $\mathbb{L}_1$ space, it is sufficient to demonstrate that $\underline{\Delta}_\tau(j) = \left(\prod_{i=0}^{j-1}\Psi(\delta_{\tau-i},\rho_{\tau-i})\right)\underline{\Pi}\left(\delta_{\tau-j},\rho_{\tau-j}\right)$ converges to zero in $\mathbb{L}_1$ at an exponential rate as $j \to +\infty$. Given the independence between δ_τ and ρ_τ, we obtain:

$$E\left\{\left|\underline{\Delta}_\tau(j)\right|\right\} = E\left\{\left|\left(\prod_{i=0}^{j-1}\Psi(\delta_{\tau-i},\rho_{\tau-i})\right)\underline{\Pi}\left(\delta_{\tau-j},\rho_{\tau-j}\right)\right|\right\} \leq Q\mathbb{M}^j(\Psi)\underline{\Lambda}(\underline{\omega}(\rho)),$$

where Q represents the block matrix $\left(I_{(m)}\vdots....\vdots I_{(m)}\right)_{m\times me}$, and $\underline{\Lambda}(\Gamma) = ((\lambda(1)\Gamma(1))', ..., (\lambda(d)\Gamma(d))')$ for any collection of non-random matrices $\Gamma := \{\Gamma(k), k \in \mathbb{E}\}$ with $\underline{\omega}(\rho) = \left(\underline{\omega}_k(\rho), k \in \mathbb{E}\right)$ and $\underline{\omega}_k(\rho) = E\left\{\left|\underline{\Pi}(k,\rho_1)\right|\right\}$. To proceed, we consider the notation $|W| := (|W_{lk}|)$ and the $\|.\|$ norm, which is chosen such that $\|W\| \leq \|\|W\|\|$, with $\underline{1}$ denoting the vector with all elements being ones. Consequently, we have:

$$\begin{aligned} E\left\{\left\|\underline{\Delta}_\tau(j)\right\|\right\} &\leq \text{Trace}\left(E\left\{\left|\underline{\Delta}_\tau(j)\underline{1}'\right|\right\}\right) \\ &\leq \left\|Q\mathbb{M}^j(\Psi)\underline{\Lambda}(\underline{\omega}(\rho))\right\| \\ &\leq \|Q\|\left\|\mathbb{M}^j(\Psi)\right\|\left\|\underline{\Lambda}(\underline{\omega}(\rho))\right\|. \end{aligned}$$

As a result of Condition (2.e), and by applying the Jordan decomposition, $\underline{\Delta}_\tau(j)$ converges to zero in $\mathbb{L}_1$ at an exponential rate as $j \to +\infty$ for all τ. Therefore, (2.b) serves as a solution to (2.a) in $\mathbb{L}_1$ and almost surely. The remaining proof follows using identical methodology to Bibi and Ghezal [22]. □

Example 2.2. *Table 2 outlines Condition* (2.*d*) *for the boundedness of expectation of square T_τ in certain instances of the MS-TBLG model.*

Table 2. Summary of Condition (2.e) for the bounded expectation of T_τ^2 across different models.

Models	Condition (2.e)	State: $r_1 = r_2 = 1$
MS-TBLG	$\rho^*(\mathbb{M}(\Psi)) < 1$	$\rho^*\left(\mathbb{P}\left(E\left\{\left\|p_1^{(1)}(.)\rho_1^{+2} + p_1^{(2)}(.)\rho_1^{-2} + s_1^{(1)}(.)\rho_1^{+} + s_1^{(2)}(.)\rho_1^{-} + q_1(.)\right\|\right\}\right)\right) < 1$
TBLG	$\rho^*(E\{\|\Psi(1,\rho_1)\|\}) < 1$	$E\left\{\left\|p_1^{(1)}(1)\rho_1^{+2} + p_1^{(2)}(1)\rho_1^{-2} + s_1^{(1)}(1)\rho_1^{+} + s_1^{(2)}(1)\rho_1^{-} + q_1(1)\right\|\right\} < 1$
MS-BLG	$\rho^*\left(\mathbb{M}(\widehat{\Psi})\right) < 1^{(*)}$	$\rho^*\left(\mathbb{P}\left(E\left\{\left\|p_1^{(1)}(.)\rho_1^{2} + s_1^{(1)}(.)\rho_1 + q_1(.)\right\|\right\}\right)\right) < 1$
Independent MS-TBLG	$\rho^*(E\{\|\Psi(\delta_1,\rho_1)\|\}) < 1$	$\sum_{k=1}^{e}\lambda(k)E\left\{\left\|p_1^{(1)}(k)\rho_1^{+2} + p_1^{(2)}(k)\rho_1^{-2} + s_1^{(1)}(k)\rho_1^{+} + s_1^{(2)}(k)\rho_1^{-} + q_1(k)\right\|\right\} < 1$
MS-GARCH	$\rho^*\left(\mathbb{M}(\widetilde{\Psi})\right) < 1^{(**)}$	$\rho^*\left(\mathbb{P}\left(E\left\{p_1^{(1)}(.)\rho_1^{2} + q_1(.)\right\}\right)\right) < 1$

$^{(*)}\ \widehat{\Psi} := \left(E\left\{\left|\widehat{\Psi}(k,\rho_1)\right|\right\}, k \in \mathbb{E}\right)$ where $\widehat{\Psi}(\delta_\tau,\rho_\tau) = \begin{pmatrix} p_{r_2}\left(\delta_\tau,\rho_\tau^2\right) & \widetilde{Q}(\delta_\tau)\rho_\tau^2 & s_{r_1\wedge r_2}(\delta_\tau)\rho_\tau^2 \\ p_{r_2}(\delta_\tau) & Q(\delta_\tau) & s_{r_1\wedge r_2}(\delta_\tau) \\ p_{r_2}(\delta_\tau)\rho_\tau & \widetilde{Q}(\delta_\tau)\rho_\tau & s_{r_1\wedge r_2}(\delta_\tau,\rho_\tau) \end{pmatrix}$,

$$f_s(\delta_\tau,\rho_\tau) = \begin{pmatrix} f_1^{(1)}(\delta_\tau)\rho_\tau & ... & f_s^{(1)}(\delta_\tau)\rho_\tau \\ 1 & ... & 0 \\ \vdots & \ddots & \vdots \\ 0 & ...1 & 0 \end{pmatrix}, Q(\delta_\tau) = \begin{pmatrix} q_1(\delta_\tau) & ... & q_{r_1}(\delta_\tau) \\ 1 & ... & 0 \\ \vdots & \ddots & \vdots \\ 0 & ...1 & 0 \end{pmatrix},$$

$$f_s(\delta_\tau) = \begin{pmatrix} f_1^{(1)}(\delta_\tau) & ... & f_s^{(1)}(\delta_\tau) \\ 0 & ... & 0 \\ \vdots & \ddots & \vdots \\ 0 & ...0 & 0 \end{pmatrix}, \widetilde{Q}(\delta_\tau) = \begin{pmatrix} q_1(\delta_\tau) & ... & q_{r_1}(\delta_\tau) \\ 0 & ... & 0 \\ \vdots & \ddots & \vdots \\ 0 & ... & 0 \end{pmatrix}.$$

$^{(**)}\ \widetilde{\Psi} := \left(E\left\{\left|\widetilde{\Psi}(k,\rho_1)\right|\right\}, k \in \mathbb{E}\right)$ where $\widetilde{\Psi}(\delta_\tau,\rho_\tau) = \begin{pmatrix} p_{r_2}\left(\delta_\tau,\rho_\tau^2\right) & \widetilde{Q}(\delta_\tau)\rho_\tau^2 \\ p_{r_2}(\delta_\tau) & Q(\delta_\tau) \end{pmatrix}$.

3. Moment and covariance of the power process in MS-TBLG models

Understanding the moment properties of the power process within MS-TBLG models is crucial for advancing the analysis and application of these models. The condition outlined in Theorem 2.2 provides a foundational framework for ensuring a stationary solution. This framework can encompass higher-order moments.

Theorem 3.1. *For Eq* (2.a)*, we presume the conditions are explicitly fulfilled if* $(\rho_\tau)_{\tau\in\mathbb{Z}}$ *adheres to a Gaussian distribution, applicable for any integer* $l-2\geq 0$*: "the expectation of* ρ_τ *raised to the power of* $2l$*, which is finite, and the expectation of* ρ_τ *raised to the power of* j *equal zero for any odd positive integer* j *less than* $2l$*". Suppose the spectral radius condition:*

$$\rho^*\left(\mathbb{M}(\Psi^{(l)})\right)<1, \tag{2.g}$$

is satisfied, where $\Psi^{(l)}:=\left(E\left\{\left|\Psi^{\otimes l}(k,\rho_\tau)\right|\right\},k\in\mathbb{E}\right)$ *defines the regime-wise average of the absolute matrix. Under these conditions, Eqs (1.a)-(1.e) admit a unique strictly stationary solution. This solution, represented by the series for* $\underline{\Upsilon}_\tau$ *as defined in* (2.b)*, converges almost surely in an absolute sense, as well as in the* $\mathbb{L}_l$ *space. Additionally, it accommodates moments up to the* $l-$*th order.*

Proof. To establish the conditions for the existence of higher-order moments, we start with the decomposition (2.f). For any integer $l-2\geq 0$, $\underline{\Delta}_\tau^{\otimes l}(j)=\left(\prod_{i=0}^{j-1}\Psi^{\otimes l}(\delta_{\tau-i},\rho_{\tau-i})\right)\underline{\Pi}^{\otimes l}\left(\delta_{\tau-j},\rho_{\tau-j}\right)$. Consequently, we have $E\left\{\left|\underline{\Delta}_\tau^{\otimes l}(j)\right|\right\}=\mathbb{Q}\mathbb{M}^j(\Psi^{(l)})\underline{\Lambda}(\underline{\omega}^{(l)}(\rho))$, where $\underline{\omega}^{(l)}(\rho)=\left(\left(\underline{\omega}_k^{(l)}(\rho)\right)',k\in\mathbb{E}\right)'$ and $\underline{\omega}_k^{(l)}(\rho)=E\left\{\left|\underline{\Pi}^{\otimes l}(k,\rho_1)\right|\right\}$. This yields $\left\|\underline{\Delta}_\tau^{\otimes l}(j)\right\|_m\leq\|\mathbb{Q}\|^{1/l}\left\|\mathbb{M}^j(\Psi^{(l)})\right\|^{1/l}\left\|\underline{\Lambda}(\underline{\omega}^{(l)}(\rho))\right\|^{1/l}$. Given condition (2.g) and utilizing the Jordan decomposition, $\left\|\mathbb{M}^j(\Psi^{(l)})\right\|$ converges to zero exponentially as $j\to\infty$. Therefore, for any τ, $\sum_{j=1}^{i}\underline{\Delta}_\tau(j)$ converges to $\underline{\Upsilon}_\tau$ defined by (2.b) as $i\to\infty$. The remaining conclusions are straightforward. □

Example 3.1. *Table 3 outlines Condition* (2.g) *for the boundedness of expectation of power* T_τ^2 *in certain instances of the MS-TBLG model.*

Table 3. Summary of Condition (2.g) for the bounded expectation of T_τ^{2l} across different models.

Models	Condition (2.g)	State: $r_1 = r_2 = 1$
MS-TBLG	$\rho^*\left(\mathbb{M}(\Psi^{(l)})\right) < 1$	$\rho^*\left(\mathbb{P}\left(E\left\{\left\|p_1^{(1)}(.)(\rho_1^+)^2 + p_1^{(2)}(.)(\rho_1^-)^2 + s_1^{(1)}(.)\rho_1^+ + s_1^{(2)}(.)\rho_1^- + q_1(.)\right\|^l\right\}\right)\right) < 1$
TBLG	$\rho^*\left(E\left\{\left\|\Psi^{\otimes l}(1,\rho_1)\right\|\right\}\right) < 1$	$E\left\{\left\|p_1^{(1)}(1)(\rho_1^+)^2 + p_1^{(2)}(1)(\rho_1^-)^2 + s_1^{(1)}(1)\rho_1^+ + s_1^{(2)}(1)\rho_1^- + q_1(1)\right\|^l\right\} < 1$
MS-BLG	$\rho^*\left(\mathbb{M}(\widehat{\Psi}^{(l)})\right) < 1^{(*)}$	$\rho^*\left(\mathbb{P}\left(E\left\{\left\|p_1^{(1)}(.)\rho_1^2 + s_1^{(1)}(.)\rho_1 + q_1(.)\right\|l\right\}\right)\right) < 1$
Independent MS-TBLG	$\rho^*\left(E\left\{\left\|\Psi^{\otimes l}(\delta_1,\rho_1)\right\|\right\}\right) < 1$	$\sum_{k=1}^{e}\lambda(k)E\left\{\left\|p_1^{(1)}(k)(\rho_1^+)^2 + p_1^{(2)}(k)(\rho_1^-)^2 + s_1^{(1)}(k)\rho_1^+ + s_1^{(2)}(k)\rho_1^- + q_1(k)\right\|^l\right\} < 1$
MS-GARCH	$\rho^*\left(\mathbb{M}(\widetilde{\Psi}^{(l)})\right) < 1^{(**)}$	$\rho^*\left(\mathbb{P}\left(E\left\{\left(p_1^{(1)}(.)\rho_1^2 + q_1(.)\right)^l\right\}\right)\right) < 1$

$^{(*)}\ \widehat{\Psi}^{(l)} := \left(E\left\{\left|\widehat{\Psi}^{\otimes l}(k,\rho_1)\right|\right\}, k \in \mathbb{E}\right)$, $^{(**)}\ \widetilde{\Psi}^{(l)} := \left(E\left\{\widetilde{\Psi}^{\otimes l}(k,\rho_1)\right\}, k \in \mathbb{E}\right)$.

The following proposition presents the explicit formula for the $(4l)^{th}-$order moment and covariance of power processes in the MS-TBLG model.

Proposition 3.1. *Consider the MS-TBLG process defined by Eqs (1.a)–(1.e) as represented in (2.a). Suppose that (2.g) holds and that $E\left\{\rho_1^{4l}\right\} < \infty$. The mean and covariance of $\left(T_\tau^{2l}\right)_\tau$ are given by:*

$$E\left\{T_\tau^{2l}\right\} = \left(\underline{L}^{\otimes 2l}\right)' Q\left(I_{(.)} - \mathbb{M}\left(\varpi^{(4l,4l)}\right)\right)^{-1}\sum_{n=0}^{2l-1}\mathbb{M}\left(\varpi^{(2n,4l)}\right)\underline{\Lambda}\left(\underline{A}_{\underline{\Upsilon}}^{(2n)}\right),$$

and for $m \geq 1$,

$$Cov\left(T_\tau^{2l}, T_{\tau-m}^{2l}\right) = \left(\underline{L}^{\otimes 4l}\right)'\left(Q\vdots\mathbf{O}\vdots\ldots\vdots\mathbf{O}\vdots - \left(E\left\{\underline{\Upsilon}_\tau^{\otimes 2l}\right\}\otimes Q\right)\right)\left(F^{(2l)}\right)^m\begin{pmatrix}\underline{\Lambda}\left(\underline{A}_{\underline{\Upsilon}}^{(4l)}\right)\\ \underline{\Lambda}\left(\underline{A}_{\underline{\Upsilon}}^{(4l-2)}\right)\\ \vdots\\ \underline{\Lambda}\left(\underline{A}_{\underline{\Upsilon}}^{(2l)}\right)\end{pmatrix},$$

where $\underline{\Lambda}\left(\underline{A}_{\underline{\Upsilon}}^{(4l)}\right) = \left(I_{(.)} - \mathbb{M}\left(\varpi^{(4l,4l)}\right)\right)^{-1}\sum_{n=0}^{2l-1}\mathbb{M}\left(\varpi^{(2n,4l)}\right)\underline{\Lambda}\left(\underline{A}_{\underline{\Upsilon}}^{(2n)}\right)$.

Proof. Define the matrices $\varpi_{\delta_\tau}^{(n,2l)}(\rho_\tau)$, $n = 0, ..., 2l$, as follows:

$$\underline{\Upsilon}_\tau^{\otimes 2l} = \left(\Psi(\delta_\tau,\rho_\tau)\underline{\Upsilon}_{\tau-1} + \underline{\Pi}(\delta_\tau,\rho_\tau)\right)^{\otimes 2l} = \sum_{n=0}^{2l}\varpi_{\delta_\tau}^{(n,2l)}(\rho_\tau)\underline{\Upsilon}_{\tau-1}^{\otimes n},$$

where $\varpi_{\delta_\tau}^{(n,2l)}(\rho_\tau) = \sum_{\sum_{j=1}^{2l} n_j = n, n_j\in\{0,1\}}\left(\Psi^{\otimes n_1}(\delta_\tau,\rho_\tau)\otimes\underline{\Pi}^{\otimes(1-n_1)}(\delta_\tau,\rho_\tau)\right)\otimes\cdots\otimes\left(\Psi^{\otimes n_{2l}}(\delta_\tau,\rho_\tau)\otimes\underline{\Pi}^{\otimes(1-n_{2l})}(\delta_\tau,\rho_\tau)\right)$.

Next, define $\underline{A}_{\underline{\Upsilon}}^{(2l)} := \left(E\left\{\underline{\Upsilon}_\tau^{\otimes 2l}\middle|\,\delta_\tau = s\right\}, s \in \mathbb{E}\right)$, $\underline{A}_{\underline{\Upsilon}}^{(2n,2l)}(m) := \left(E\left\{\underline{\Upsilon}_\tau^{\otimes 2n}\otimes\underline{\Upsilon}_{\tau-m}^{\otimes 2l}\middle|\,\delta_\tau = s\right\}, s \in \mathbb{E}\right)$, and

$\varpi^{(n,l)} := \left(E\left\{\varpi_s^{(n,l)}(\rho_\tau)\right\}, s \in \mathbb{E}\right)$. It follows that:

$$\begin{aligned}
\underline{\Lambda}\left(\underline{A}_{\underline{\Upsilon}}^{(4l)}\right) &= \sum_{n=0}^{2l} \mathbb{M}\left(\varpi^{(2n,4l)}\right)\underline{\Lambda}\left(\underline{A}_{\underline{\Upsilon}}^{(2n)}\right) \\
&= \mathbb{M}\left(\varpi^{(4l,4l)}\right)\underline{\Lambda}\left(\underline{A}_{\underline{\Upsilon}}^{(4l)}\right) + \sum_{n=0}^{2l-1} \mathbb{M}\left(\varpi^{(2n,4l)}\right)\underline{\Lambda}\left(\underline{A}_{\underline{\Upsilon}}^{(2n)}\right), \\
\underline{\Lambda}\left(\underline{A}_{\underline{\Upsilon}}^{(2n,2l)}(m)\right) &= \sum_{t=0}^{n} \mathbb{M}\left(\omega^{(2t,2l)}\right)\underline{\Lambda}\left(\underline{A}_{\underline{\Upsilon}}^{(2t,2l)}(m-1)\right),
\end{aligned}$$

where $\omega^{(n,l)} = \varpi^{(n,l)} \otimes I_{(.)}$. Additionally, we have:

$$\begin{aligned}
G^{(2l)}(m) &= \left(\left(\underline{\Lambda}\left(\underline{A}_{\underline{\Upsilon}}^{(2l,2l)}(m)\right)\right)', \left(\underline{\Lambda}\left(\underline{A}_{\underline{\Upsilon}}^{(2(l-1),2l)}(m)\right)\right)', ..., \left(\underline{\Lambda}\left(\underline{A}_{\underline{\Upsilon}}^{(0,2l)}(m)\right)\right)'\right)' \\
&= \begin{pmatrix}
\mathbb{M}\left(\omega^{(0,2l)}\right) & \mathbb{M}\left(\omega^{(2,2l)}\right) & \cdots & \cdots & \mathbb{M}\left(\omega^{(2l,2l)}\right) \\
O & \mathbb{M}\left(\omega^{(0,2l-2)}\right) & \cdots & \cdots & \mathbb{M}\left(\omega^{(2l-2,2l-2)}\right) \\
\vdots & \ddots & \ddots & \cdots & \vdots \\
\vdots & \ddots & \ddots & \mathbb{M}\left(\omega^{(0,2)}\right) & \mathbb{M}\left(\omega^{(2,2)}\right) \\
O & \cdots & \cdots & O & \mathbb{M}\left(I_{(.)}\right)
\end{pmatrix} G^{(2l)}(m-1) \\
&= F^{(2l)} G^{(2l)}(m-1), \text{ for } m \geq 1
\end{aligned}$$

in which O is the null matrix with appropriate dimensions, and $I_{(.)}$ is the identity matrix with appropriate dimensions. For $m \geq 1$,

$$\begin{aligned}
Cov\left(T_\tau^{2l}, T_{\tau-m}^{2l}\right) &= \left(\underline{L}^{\otimes 4l}\right)'\left(E\left\{\underline{\Upsilon}_\tau^{\otimes 2l} \otimes \underline{\Upsilon}_{\tau-m}^{\otimes 2l}\right\} - E\left\{\underline{\Upsilon}_\tau^{\otimes 2l}\right\} \otimes E\left\{\underline{\Upsilon}_{\tau-m}^{\otimes 2l}\right\}\right) \\
&= \left(\underline{L}^{\otimes 4l}\right)'\left(Q\underline{\Lambda}\left(\underline{A}_{\underline{\Upsilon}}^{(2l,2l)}(m)\right) - \left(E\left\{\underline{\Upsilon}_\tau^{\otimes 2l}\right\} \otimes Q\right)\underline{\Lambda}\left(\underline{A}_{\underline{\Upsilon}}^{(0,2l)}(m)\right)\right) \\
&= \left(\underline{L}^{\otimes 4l}\right)'\left(Q\vdots\mathbf{O}\vdots\ldots\vdots\mathbf{O}\vdots - \left(E\left\{\underline{\Upsilon}_\tau^{\otimes 2l}\right\} \otimes Q\right)\right)G^{(2l)}(m) \\
&= \left(\underline{L}^{\otimes 4l}\right)'\left(Q\vdots\mathbf{O}\vdots\ldots\vdots\mathbf{O}\vdots - \left(E\left\{\underline{\Upsilon}_\tau^{\otimes 2l}\right\} \otimes Q\right)\right)\left(F^{(2l)}\right)^m G^{(2l)}(0).
\end{aligned}$$

The proof is thus concluded. □

4. Generalized method of moments estimation

Estimating Markov-switching models is notoriously challenging due to the recursive structure of the volatility equation. At each point in time, the current volatility relies on the entire history of regimes, which are dictated by an unobservable Markov chain. This dependency creates an exponential increase in the number of possible regime paths, evaluating the likelihood function computationally infeasible as time progresses. To circumvent these difficulties, various innovative estimation methods have emerged in the literature. Notably, the GMM has proven to be a robust and versatile tool. The GMM utilizes moment conditions derived from the data to generate estimators that are both consistent and efficient, even in the presence of complex dependencies and heteroskedasticity. In this study, we focus on

leveraging the GMM to estimate MS-TBLG models by using the covariance functions of the squared process's powers.

Building on the foundational work of Francq and Zakoian [24], this paper illustrates how the derived covariance functions can be effectively applied to fit general MS-TBLG models to econometric datasets. We provide a succinct review of the fundamental GMM tools necessary for statistical inference, directing those interested in a detailed mathematical framework to Harris and Mátyás [25].

Consider a scenario where the orders r_1, r_2, and the number of regimes e, are predefined. The parameters that need to be estimated are consolidated into a vector $\underline{\vartheta}$, which is defined as the concatenation of $\underline{\vartheta}_1$ through $\underline{\vartheta}_e$, which resides within the parameter space Θ. Each $\underline{\theta}_i$ is further detailed as $p_0(i)$, $p_u^{(1)}(i)$, $p_u^{(2)}(i)$, $q_v(i)$, $s_w^{(1)}(i)$, $s_w^{(2)}(i)$, λ_{ij}, with $u = 1, ..., r_2$, $v = 1, ..., r_1$, $w = 1, ..., r_1 \wedge r_2$, $i, j \in \mathbb{E}$, and $i \neq j$. The true parameter vector, denoted by $\underline{\vartheta}_0$, is unknown and requires estimation. The orthogonality condition utilized is expressed by the vectorial equation $E_{\underline{\theta}_0}\left\{\Sigma\left(\underline{\vartheta}, \underline{T}_\tau\right)\right\} = 0$ where $\underline{T}'_\tau := \left(\underline{T}_\tau, \underline{T}_{\tau-1}..., \underline{T}_{\tau-\alpha}\right)$ and the components of $\Sigma\left(\underline{\vartheta}, \underline{T}_\tau\right)$ are $T_\tau^2 - E_{\underline{\theta}}\left\{T_\tau^2\right\}$ and $T_\tau^{2l}T_{\tau-k}^{2l} - E_{\underline{\theta}}\left\{T_\tau^{2l}T_{\tau-k}^{2l}\right\}$, $k = 0, ..., h_l$, $l = 1, ..., L$, and $H = \max_l h_l$. Make sure that L and α are chosen such that the orthogonality conditions and the moment existence conditions, as established by Theorem 3.1, are satisfied. For this purpose, consider a realization of length $m \geq \alpha$, where α is a given lag, $\{T_1, ..., T_m\}$ is from the unique, causal, strictly stationary, and ergodic solutions of Eqs (1.a) and (1.e), the GMM estimator $\widehat{\underline{\vartheta}}_m$ is derived by minimizing the objective function $O_m\left(\underline{\vartheta}\right)$ over $\underline{\vartheta} \in \Theta : O_m\left(\underline{\vartheta}\right) = Z'_m\left(\underline{\vartheta}\right) V_m Z_m\left(\underline{\vartheta}\right)$, where $Z_m\left(\underline{\theta}\right) = \frac{1}{m-H}\sum_{\tau=H+1}^{m}\Sigma\left(\underline{\vartheta}, \underline{T}_\tau\right)$, and V_m represents a sequence of positive definite weighting matrices that converge to a symmetric and invertible W which is non-random. Under the condition $\rho^*\left(\mathbb{M}(\Psi^{(2L)})\right) < 1$ for each $\underline{\vartheta} \in \Theta$, the process $\left(\Sigma\left(\underline{\vartheta}, \underline{T}_\tau\right)\right)_{\tau\in\mathbb{Z}}$ is stationary, ergodic, and satisfies $\left\|E_{\underline{\theta}_0}\left\{\Sigma\left(\underline{\vartheta}, \underline{T}_\tau\right)\right\}\right\| < +\infty$. Consequently, almost surely, $\frac{1}{m-H}\sum_{\tau=H+1}^{m}\Sigma\left(\underline{\vartheta}, \underline{T}_\tau\right) \to E_{\underline{\theta}_0}\left\{\Sigma\left(\underline{\vartheta}, \underline{T}_\tau\right)\right\}$. As a result, the estimator $\widehat{\underline{\vartheta}}_m$ is consistent and asymptotically normal, provided that suitable regularity conditions are met (as detailed, for example, by Harris and Mátyás [25]): $\sqrt{m}\left(\widehat{\underline{\vartheta}}_m - \underline{\vartheta}_0\right) \rightsquigarrow \mathcal{N}(0, Y)$, where $Y := C^{-1}\left\{\nabla_{\underline{\vartheta}'}\underline{\Xi}\left(\underline{\vartheta}\right) VDV\nabla_{\underline{\vartheta}}\underline{\Xi}\left(\underline{\vartheta}\right)\right\}C^{-1}$, $C = \nabla_{\underline{\vartheta}'}\underline{\Xi}\left(\underline{\vartheta}\right) V\underline{\Xi}\left(\underline{\vartheta}\right)$, $D = \lim_m Var_{\underline{\vartheta}_0}\left(Z_m\left(\underline{\theta}\right)\right)$ where $\underline{\Xi}\left(\underline{\vartheta}\right) = E_{\underline{\theta}_0}\left\{f\Sigma\left(\underline{\vartheta}, \underline{T}_\tau\right)\right\}$.

Remark 4.1. *The optimal choice of the weighting matrix V in GMM estimation significantly affects the asymptotic efficiency of the estimator $\widehat{\underline{\vartheta}}_m$. Selecting $V = U^{-1}$, where U is the covariance matrix of the moment conditions, minimizes the asymptotic variance of $\widehat{\underline{\vartheta}}_m$. Accurate estimation of U is crucial for constructing reliable confidence intervals and performing valid statistical tests. The Newey–West estimator is commonly used to approximate U, with kernels such as Bartlett and Parzen ensuring positive semi-definite estimates.*

Remark 4.2. *The proposed MS-TBLG model is classified as a path-dependent model due to the dynamic interaction between its threshold component and Markovian regime-switching mechanism. While such models typically require advanced estimation techniques like MCMC—as in the work of Bauwens et al. [26]—this study introduces an alternative GMM-based methodology that is both computationally efficient and capable of capturing the model's intrinsic features without the need to trace all possible latent state paths. Our approach is grounded in a rigorous system of moment conditions, specifically tailored to handle the structural complexity of the MS-TBLG framework. It*

also builds on key theoretical insights from prior contributions, such as Gray [7] and Haas et al. [9]. Notably, this methodology circumvents the practical difficulties associated with traditional maximum likelihood (ML) estimation, as underscored by Francq and Zakoian [24], making it a compelling choice for applied contexts while preserving the necessary statistical precision.

5. Monte Carlo experiments

Monte Carlo experiments were conducted to evaluate the performance of the MS-TBLG model in estimating the true parameters of the model. Two different sample sizes, $m = 2500$ and $m = 4500$, were used to analyze the effect of sample size on the accuracy of the estimates. A total of 1000 simulations were performed for each sample size. Table 4 presents the estimated parameters, their true values, and standard deviations (shown in parentheses).

Table 4. Parameter estimates for the MS-TBLG model from Monte Carlo simulations.

Parameters	Tv	$m = 2500$		$m = 4500$	
$\widehat{\underline{p}}_0$	1.00	0.9428	(0.0618)	0.9623	(0.0475)
	1.00	0.9714	(0.0566)	0.9853	(0.0393)
$\widehat{\underline{p}}_1^{(1)}$	0.35	0.3399	(0.1087)	0.3418	(0.0918)
	0.20	0.1903	(0.0523)	0.1973	(0.0405)
$\widehat{\underline{p}}_1^{(2)}$	0.15	0.1440	(0.0465)	0.1491	(0.0372)
	0.10	0.0963	(0.0352)	0.0977	(0.0287)
$\widehat{\underline{q}}_1$	0.01	0.0400	(0.0315)	0.0299	(0.0232)
	0.00	0.0258	(0.0278)	0.0152	(0.0196)
$\widehat{\underline{s}}_1^{(1)}$	0.30	0.3186	(0.1256)	0.3132	(0.1190)
	0.14	0.1507	(0.0748)	0.1459	(0.0653)
$\widehat{\underline{s}}_1^{(2)}$	0.13	0.1334	(0.0530)	0.1326	(0.0495)
	0.09	0.0912	(0.0506)	0.0906	(0.0401)
λ_{11}	0.20	0.1902	(0.0115)	0.2021	(0.0024)
λ_{22}	0.75	0.7361	(0.0143)	0.7458	(0.0035)

The parameter estimates for $p_0(k)$ and $p_1^{(i)}(k)$, $k, i = 1, 2$, are generally close to the true values, with a slight reduction in bias as the sample size increases from 2500 to 4500. For parameter $q_1(k)$, $k = 1, 2$, there is a noticeable difference between the estimated and true values, which is expected given the small magnitude of $q_1(k)$, $k = 1, 2$. However, the standard deviations decrease as the sample size increases, indicating improved precision. The estimates for $s_1^{(1)}(k)$, $k = 1, 2$, and $s_1^{(2)}(k)$, $k = 1, 2$, also improve with larger sample sizes, as evidenced by the reduced standard deviations. Finally, the transition probabilities λ_{11} and λ_{22} are estimated very accurately, with the estimates being very close to the true values and the standard deviations being quite small. This indicates high precision in estimating these parameters, with accuracy improving further as the sample size increases.

6. Analyzing daily crude oil price fluctuations using MS-TBLG models

Oil prices are a crucial economic factor significantly impacting the global economy. These prices fluctuate daily due to various economic and political influences. This study uses MS-TBLG models to analyze the daily crude oil prices of Algeria's Sahara blend from January 2000 to September 2014, which were previously examined by Ghezal [27] via Plog GARCH models. This analysis covers descriptive statistics of the time series for prices and daily logarithmic returns, as well as an autocorrelation analysis of the returns, providing a deeper understanding of oil price fluctuations. The following tables present the descriptive statistics for the time series of crude oil prices and daily logarithmic returns and the estimated values of the coefficients $corr(re_\tau, re_{\tau-m})$.

Table 5. Summary statistics of crude oil prices and returns.

The series	Mean	SD	Median	Max	Min	Skew	Kurt	JB
(z_τ)	67.6369	34.1652	65.9200	145.5200	16.7600	0.1853	1.6521	2.96×10^2
(re_τ)	0.0003	0.0221	0.0009	0.1267	−0.1971	−0.3236	8.5952	48.10×10^2
$(\lvert re_\tau \rvert)$	0.0157	0.0154	0.0120	0.1971	0.0000	2.7190	17.1899	350.14×10^2
$\left(re_\tau^2\right)$	0.0004	0.0013	0.0001	0.0388	0.0000	11.7366	238.1221	84.657×10^5

Table 6. Estimated values of the coefficients $corr(re_\tau, re_{\tau-m})$.

Lag	1	2	3	4	5	6	7	8	9	10
$\widehat{corr}(re_\tau, re_{\tau-m})$	−0.0017	0.0027	0.0144	0.0013	−0.0058	−0.0282	0.0394	0.0027	0.0126	0.0160

The summary statistics in Table 5 reveal that the crude oil prices exhibit substantial variability, with a mean price of 67.6369 and a standard deviation of 34.1652. The log-returns re_τ have a mean close to zero, indicating that the daily returns do not show a significant upward or downward trend on average. However, the high kurtosis and JB test statistics for re_τ and re_τ^2 suggest the presence of heavy tails and potential non-normality in the returns distribution. The correlation coefficients in Table 6 indicate that the log-returns re_τ have low autocorrelation for most lags, with some exceptions at specific lags like 3 and 7. This low autocorrelation suggests that the returns series have a weak dependency structure, which is a characteristic often observed in financial time series. Moving forward, we visualize the time series of daily crude oil prices during the study period in Figure 1.

Figure 1 shows significant fluctuations in prices, with clear periods of rise and fall reflecting various economic and political influences. To further understand the dynamics, we present the sample autocorrelation of log, squared log, and absolute log returns in Figure 2.

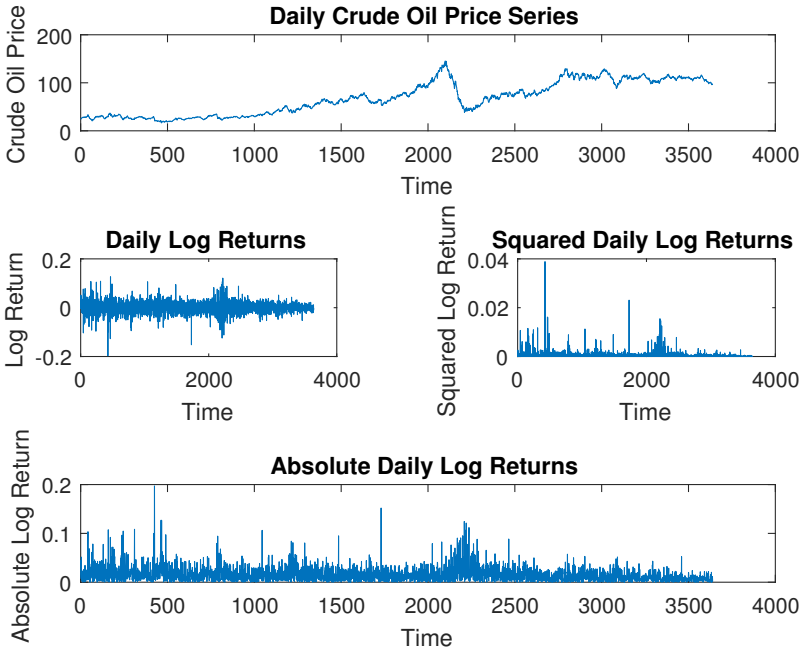

Figure 1. Daily crude oil price series.

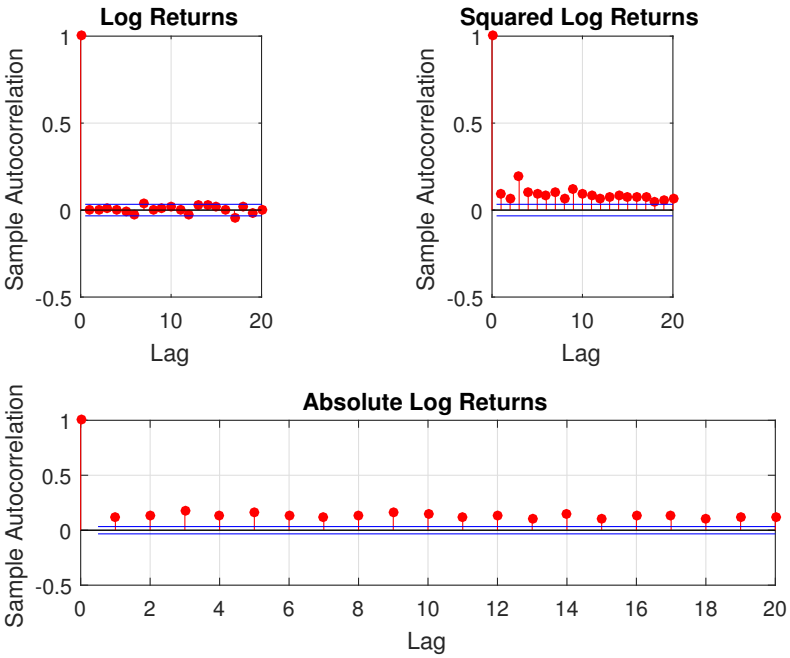

Figure 2. Sample autocorrelation of log, squared log, and absolute log returns.

Figure 2 illustrates generally low autocorrelation across different time lags, with some significant autocorrelations at specific lags possibly due to unexpected market events. Next, we examine the partial autocorrelation of daily logarithmic returns in Figure 3.

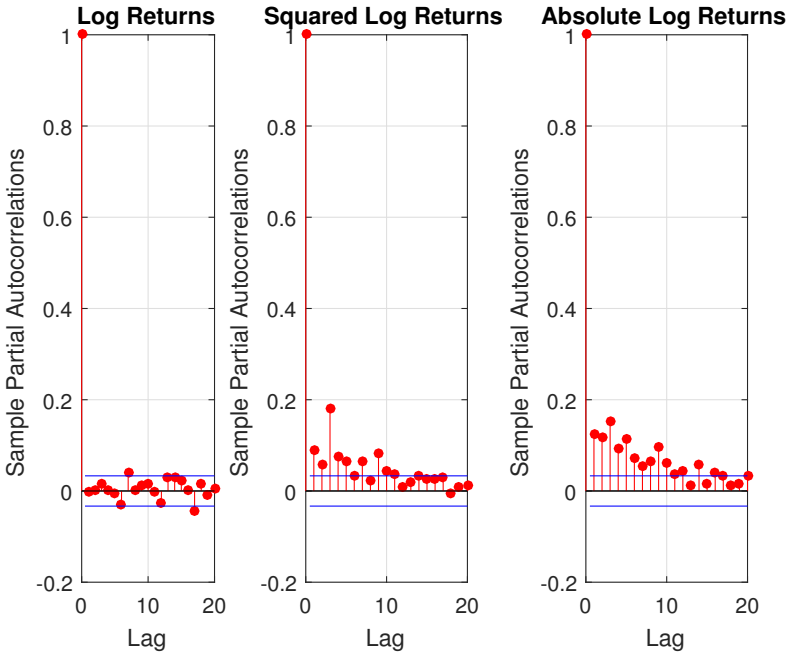

Figure 3. Partial autocorrelation of log, squared log, and absolute log returns.

Figure 3 shows that partial autocorrelation decreases rapidly with increasing lag, indicating that most effects depend primarily on near periods, consistent with financial time series properties. We now present the partial autocorrelation of the fitted $(\widetilde{re}_\tau)$ and $\left(\widetilde{re}_\tau^2\right)$ series for returns and squared returns in Figure 4.

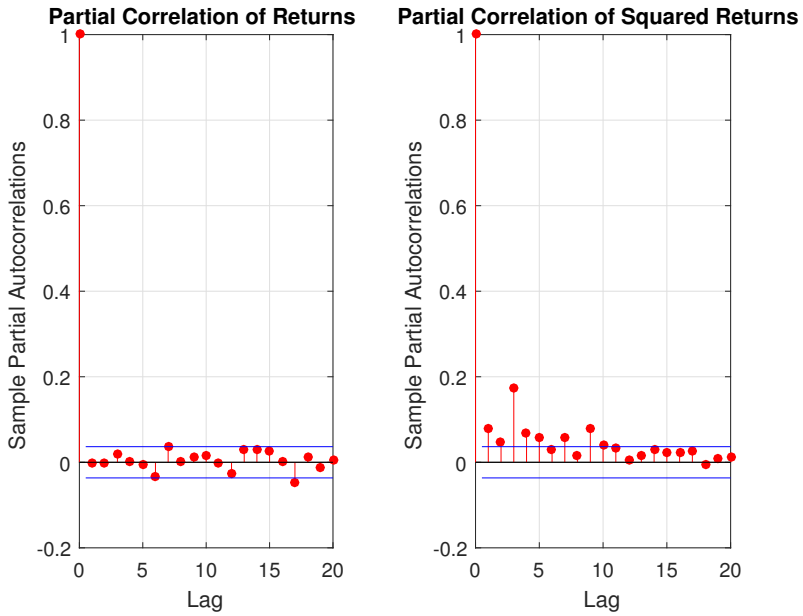

Figure 4. Partial autocorrelation of fitted series $(\widetilde{re}_\tau)$ and $\left(\widetilde{re}_\tau^2\right)$.

Figure 4 reveals patterns in the partial autocorrelation values, which could be important for understanding price fluctuation dynamics. Next, we examine the model residuals, p-values, and QQ plots in Figure 5.

Figure 5 indicates that the model residuals are well-distributed around zero, suggesting the model's adequacy in analyzing the data. The QQ plot shows that the residuals follow a normal distribution fairly well. Next, we present the news impact curves on returns in Figure 6.

Figure 6 demonstrates the positive and negative impacts of news on returns, reflecting how prices respond to various economic and political events. This comprehensive analysis provides valuable insights into the dynamics of daily crude oil price fluctuations. Lastly, to further analyze the dynamic behavior of regime shifts captured by the MS-TBLG model, we now examine the evolution of the latent state variable over time. Specifically, we report the filtered, predictive, and smoothed probabilities associated with the two Markov regimes. The results are presented in Figure 7.

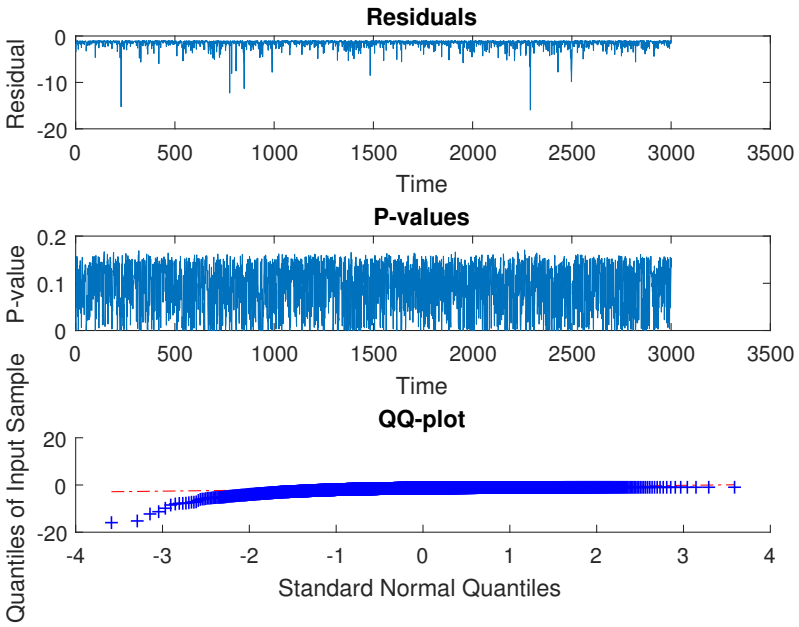

Figure 5. Residuals, p-values, and QQ plot.

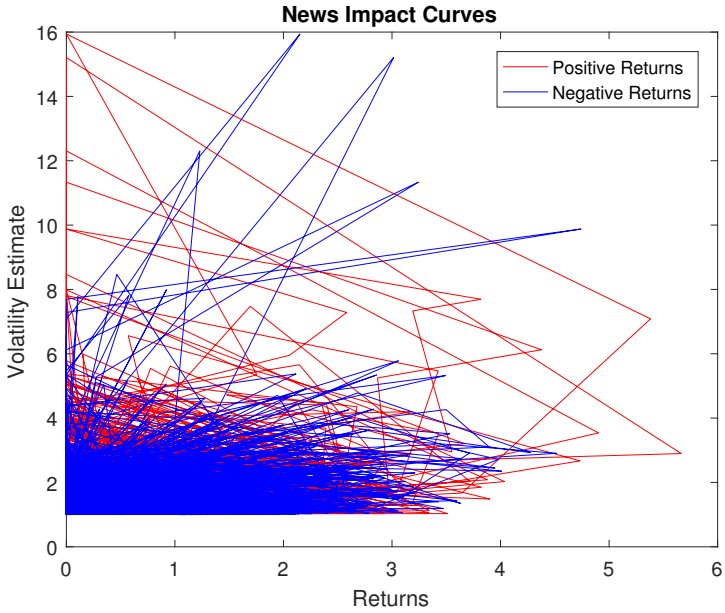

Figure 6. News impact curves.

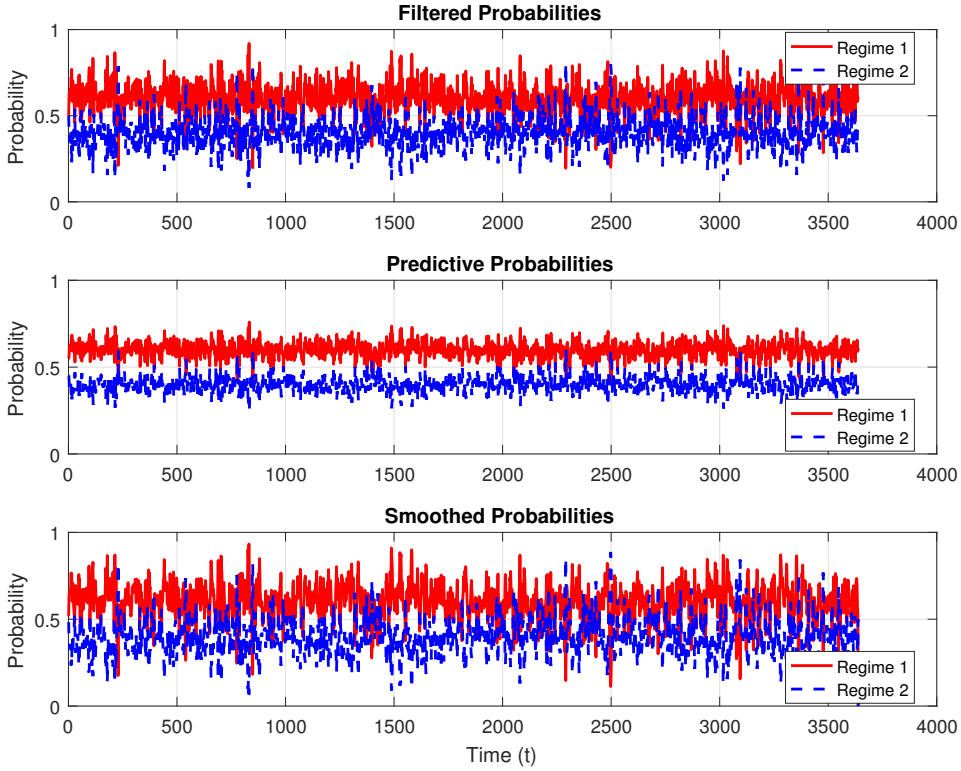

Figure 7. Filtered, predictive, and smoothed probabilities of the Markov regimes in the MS-TBLG model.

Figure 7 presents the filtered, predictive, and smoothed probability estimates from the fitted MS-TBLG model, revealing distinct regime dynamics in crude oil markets. The filtered probabilities (Panel 1) demonstrate sharp transitions between regimes, capturing instantaneous responses to market shocks and policy changes, while the predictive probabilities (Panel 2) show slightly smoother patterns due to forward-looking uncertainty. Most notably, the smoothed probabilities (Panel 3) provide the clearest perspective using full-sample information, exhibiting well-defined periods of regime persistence—particularly during times of market stress—with more pronounced transitions that highlight structural volatility shifts. Together, these probability estimates validate the MS-TBLG model's capacity to identify both transient volatility spikes and enduring regime changes, offering a nuanced understanding of crude oil return dynamics that distinguishes between short-term fluctuations and long-term structural breaks in market behavior. Furthermore, the diagnostic outcomes of the portmanteau test—specifically the Ljung–Box statistic, denoted as LBtest—summarized in Table 7, are employed to examine the null hypothesis H0: "The residuals are not autocorrelated". The test was applied over the first 100 lags, with the indicator $h = 0$ suggesting that there is insufficient evidence to reject H0, implying no significant autocorrelation. Conversely, $h = 1$ denotes the presence of significant autocorrelation (or ARCH effects), particularly when the corresponding $p-$values fall below the 1% significance threshold (i.e., p-value< 0.01). Such cases provide compelling grounds to reject the null hypothesis in favor of the alternative, indicating persistent dependence structures in the data.

Table 7. The LB test results for both the return series (re_t) and (re_t^2), segmented across lag intervals.

Lags	$\{1, ..., 39\}$	$\{40, ..., 56\}$	$\{57, ..., 100\}$
$\begin{pmatrix} h \\ p-values \end{pmatrix}$ = LB test (re_t)	$\begin{pmatrix} 1 \\ p-value \end{pmatrix} = 0.0473$	$\begin{pmatrix} 0 \\ Min-p-values \end{pmatrix} = 0.0532$	$\begin{pmatrix} 1 \\ Max-p-values \end{pmatrix} = 0.0005$
$\begin{pmatrix} h \\ p-values \end{pmatrix}$ = LB test (re_t^2)	$\begin{pmatrix} 1 \\ p-value \end{pmatrix} = 0$	$\begin{pmatrix} 1 \\ Min-p-values \end{pmatrix} = 0$	$\begin{pmatrix} 1 \\ Max-p-values \end{pmatrix} = 0$

Table 7 reports the results of the Ljung–Box portmanteau test for both the return series (re_t) and its squared values (re_t^2), across segmented lag intervals. For (re_t), the test over lags 1–39 yields a test statistic $h = 1$ with a $p-$value of 0.0473, indicating marginal evidence of autocorrelation at the 5% level, though it remains above the stricter 1% significance threshold. Over the next interval, lags 40–56, the result changes to $h = 0$, accompanied by a minimum $p-$value of 0.0532, suggesting no strong evidence to reject the null hypothesis of no autocorrelation. However, the test over lags 57–100 reverts to $h = 1$, with a maximum $p-$value as low as 0.0005, providing a strong rejection of $H0$ and signaling statistically significant structure in the residuals. In contrast, the test results for (re_t^2) are unequivocal: across all lag intervals from 1 to 100, the portmanteau test consistently reports $h = 1$, with $p-$values equal to zero. This indicates persistent and highly significant ARCH-type effects in the squared residuals, strongly supporting the presence of nonlinear conditional heteroskedasticity. Taken together, these findings highlight the importance of employing volatility models that account for higher-order dynamics, as conventional linear specifications may fail to adequately capture the complex stochastic structure of the data.

7. Conclusions

In conclusion, this paper introduces the MS-TBLG model, a significant advancement over traditional Markov-switching models by integrating threshold mechanisms to better capture complex dynamics and structural changes in financial time series. Our theoretical analysis ensures the existence of stationary, causal, and ergodic solutions, and we derive the necessary covariance functions for the power MS-TBLG model. The robustness of the GMM estimation is validated through Monte Carlo simulations, and the practical applicability of the model is demonstrated through its application to real-world data, with a particular focus on oil price dynamics.

In line with the contributions presented in this paper, several promising directions for future research can be outlined to further advance the MS-TBLG framework: (1) Incorporating the influence of external shocks, where the methodology of Zhao et al. [28] can be employed to construct geopolitical shock indices and integrate them into the model to enhance its forecasting accuracy during periods of heightened uncertainty; (2) Accounting for climate policy uncertainty by developing tailored extensions of the model capable of capturing the market implications of climate-related policy volatility, as highlighted by the findings of Zhao et al. [29]; (3) Extending the framework to a multivariate setting, enabling the analysis of joint dynamics among variables through the inclusion of cyclical components and the application of GARCH-MIDAS techniques to effectively handle mixed-frequency data; (4) Enhancing out-of-sample forecasting performance by adopting advanced evaluation tools, such as the model confidence set (MCS) and direction-of-change (DoC) metrics, to improve the reliability and robustness of long-term predictive results.

Use of Generative-AI tools declaration

The author declares he has not used Artificial Intelligence (AI) tools in the creation of this article.

Conflict of interest

The author declares no conflicts of interest in this paper.

References

1. R. F. Engle, Autoregressive conditional heteroskedasticity with estimates of the variance of United Kingdom inflation, *Econometrica*, **50** (1982), 987–1007.
2. T. Bollerslev, Generalized autoregressive conditional heteroskedasticity, *J. Econometrics*, **31** (1986), 307–327. https://doi.org/10.1016/0304-4076(86)90063-1
3. G. Storti, C. Vitale, BL-GARCH models and asymmetries in volatility, *Stat. Method. Appl.*, **12** (2003), 19–39. https://doi.org/10.1007/BF02511581
4. F. Black, Studies in stock price volatility changes, In: *Proceedings of the 1976 meeting of the business and economic statistics section*, American Statistical Association, 1976, 177–181.
5. C. Gourieroux, *ARCH models and financial applications*, New York: Springer, 1997. https://doi.org/10.1007/978-1-4612-1860-9

6. M. S. Choi, J. A. Park, S. Y. Hwang, Asymmetric GARCH processes featuring both threshold effect and bilinear structure, *Stat. Probabil. Lett.*, **82** (2012), 419–426. https://doi.org/10.1016/j.spl.2011.11.023
7. S. F. Gray, Modeling the conditional distribution of interest rates as a regime-switching process, *J. Financ. Econ.*, **42** (1996), 27–62. https://doi.org/10.1016/0304-405X(96)00875-6
8. F. Klaassen, Improving GARCH volatility forecasts with regime-switching GARCH, *Empir. Econ.*, **27** (2002), 363–394. https://doi.org/10.1007/s001810100100
9. M. Haas, S. Mittnik, M. S. Paolella, A new approach to Markov-switching GARCH models, *J. Financ. Econom.*, **2** (2004), 493–530. https://doi.org/10.1093/jjfinec/nbh020
10. A. Abramson. I. Cohen, On the stationarity of Markov-switching GARCH processes, *Econom. Theor.*, **23** (2007), 485–500. https://doi.org/10.1017/S0266466607070211
11. M. Cavicchioli, Markov switching GARCH models: higher order moments, kurtosis measures and volatility evaluation in recessions and pandemic, *J. Bus. Econ. Stat.*, **40** (2022), 1772–1783. https://doi.org/10.1080/07350015.2021.1974459
12. M. Cavicchioli, Higher order moments of Markov switching VARMA models, *Econom. Theor.*, **33** (2017), 1502–1515. https://doi.org/10.1017/S0266466616000438
13. A. Ghezal, O. Alzeley, Probabilistic properties and estimation methods for periodic threshold autoregressive stochastic volatility, *AIMS Math.*, **9** (2024), 11805–11832. https://doi.org/10.3934/math.2024578
14. A. Ghezal, M. Balegh, I. Zemmouri, Markov-switching threshold stochastic volatility models with regime changes, *AIMS Math.*, **9** (2024), 3895–3910. https://doi.org/10.3934/math.2024192
15. A. Ghezal, Spectral representation of Markov-switching bilinear processes, *São Paulo J. Math. Sci.*, **18** (2024), 459–479. https://doi.org/10.1007/s40863-023-00380-w
16. A. Ghezal, I. Zemmouri, On the Markov-switching autoregressive stochastic volatility processes, *SeMA*, **81** (2024), 413–427. https://doi.org/10.1007/s40324-023-00329-1
17. A. Ghezal, I. Zemmouri, On Markov-switching asymmetric log GARCH models: stationarity and estimation, *Filomat*, **37** (2023), 9879–9897. https://doi.org/10.2298/FIL2329879G
18. A. Ghezal, I. Zemmouri, $M-$estimation in periodic threshold GARCH models: consistency and asymptotic normality, *Miskolc Math. Notes*, **26** (2025), 229–242. https://doi.org/10.18514/MMN.2025.4747
19. A. Bibi, A. Ghezal, Markov-switching BILINEAR-GARCH models: structure and estimation, *Commun. Stat.-Theor. Meth.*, **47** (2018), 307–323. https://doi.org/10.1080/03610926.2017.1303732
20. A. Aknouche, N. Rabehi, On an independent and identically distributed mixture bilinear time-series model, *J. Time Ser. Anal.*, **31** (2010), 113–131. https://doi.org/10.1111/j.1467-9892.2009.00649.x
21. P. Bougerol, N. Picard, Strict stationarity of generalized autoregressive processes, *Ann. Probab.*, **20** (1992), 1714–1730. https://doi.org/10.1214/aop/1176989526
22. A. Bibi, A. Ghezal, On the Markov-switching bilinear processes: stationarity, higher-order moments and $\beta-$mixing, *Stochastics*, **87** (2015), 919–945. https://doi.org/10.1080/17442508.2015.1019881

23. A. Ghezal, M. Cavicchioli, I. Zemmouri, On the existence of stationary threshold bilinear processes, *Stat. Papers*, **65** (2024), 3739–3767. https://doi.org/10.1007/s00362-024-01539-z

24. C. Francq, J. M. Zakoïan, Stationarity of multivariate Markov-switching ARMA models, *J. Econometrics*, **102** (2001), 339–364. https://doi.org/10.1016/S0304-4076(01)00057-4

25. D. Harris, L. Mátyás, Introduction to the generalized method of moments estimation, In: *Generalized method of moments estimation*, Cambridge: University Press, 1999, 3–30. https://doi.org/10.1017/CBO9780511625848.002

26. L. Bauwens, A. Preminger, J. V. K. Rombouts, Theory and inference for a Markov switching GARCH model, *Economet. J.*, **13** (2010), 218–244. https://doi.org/10.1111/j.1368-423X.2009.00307.x

27. A. Ghezal, QMLE for periodic time-varying asymmetric log GARCH models, *Commun. Math. Stat.*, **9** (2021), 273–297. https://doi.org/10.1007/s40304-019-00193-4

28. C. Liang, L. Wang, D. Duong, More attention and better volatility forecast accuracy: How does war attention affect stock volatility predictability?, *J. Econ. Behav. Organ.*, **218** (2024), 1–19. https://doi.org/10.1016/j.jebo.2023.12.009

29. C. Liang, M. Umar, F. Ma, T. L. D. Huynh, Climate policy uncertainty and world renewable energy index volatility forecasting, *Technol. Forecast. Soc.*, **182** (2022), 121810. https://doi.org/10.1016/j.techfore.2022.121810

AIMS Press